energy&fuels

Article

pubs.acs.org/EF

Mechanism of Methane Chemical Looping Combustion with Hematite Promoted with CeO_2

Duane D. Miller*[,†,‡] and Ranjani Siriwardane[†]

[†]National Energy Technology Laboratory (NETL), United States Department of Energy (U.S. DOE), 3610 Collins Ferry Road, Post Office Box 880, Morgantown, West Virginia 26507-0880, United States

[‡]URS Corporation, 3610 Collins Ferry Road, Morgantown, West Virginia 26507-0880, United States

ABSTRACT: Chemical looping combustion (CLC) is a promising technology for fossil fuel combustion that produces sequestration-ready CO_2 stream, reducing the energy penalty of CO_2 separation from flue gases. An effective oxygen carrier for CLC will readily react with the fuel gas and will be reoxidized upon contact with oxygen. This study investigated the development of a CeO_2-promoted Fe_2O_3–hematite oxygen carrier suitable for the methane CLC process. Composition of CeO_2 is between 5 and 25 wt % and is lower than what is generally used for supports in Fe_2O_3 carrier preparations. The incorporation of CeO_2 to the natural ore hematite strongly modifies the reduction behavior in comparison to that of CeO_2 and hematite alone. Temperature-programmed reaction studies revealed that the addition of even 5 wt % CeO_2 enhances the reaction capacity of the Fe_2O_3 oxygen carrier by promoting the decomposition and partial oxidation of methane. Fixed-bed reactor data showed that the 5 wt % cerium oxides with 95 wt % iron oxide produce 2 times as much carbon dioxide in comparison to the sum of carbon dioxide produced when the oxides were tested separately. This effect is likely due to the reaction of CeO_2 with methane forming intermediates, which are reactive for extracting oxygen from Fe_2O_3 at a considerably faster rate than the rate of the direct reaction of Fe_2O_3 with methane. These studies reveal that 5 wt % CeO_2/Fe_2O_3 gives stable conversions over 15 reduction/oxidation cycles. Lab-scale reactor studies (pulsed mode) suggest the methane reacts initially with CeO_2 lattice oxygen to form partial oxidation products ($CO + H_2$), which continue to react with oxygen from neighboring Fe_2O_3, leading to its complete oxidation to form CO_2. The reduced cerium oxide promotes the methane decomposition reaction to form $C + H_2$, which continue to react with Fe_2O_3/Fe_3O_4 to form CO/CO_2 and H_2O. This mechanism is supported by the characterization studies, which also suggest that the formation of carbonaceous intermediates may affect the reaction rate and selectivity of the oxygen carrier.

1. INTRODUCTION

The chemical looping combustion (CLC) system is a technique by which a concentrated CO_2 stream is produced during combustion when the gaseous fuel is introduced to the fuel reactor containing an oxygen-rich metal oxide (Me_xO_y). The oxide proceeds to react with the fuel, producing a reduced oxygen carrier (Me_xO_{y-1}). The major challenge with CLC using Fe_2O_3[1] and natural ores[2−5] is the release of adequate amounts of oxygen from the oxygen carrier during the CLC reduction cycle. A low oxygen capacity will result in a larger amount of solids transfer, contributing to a significant increase in the CLC reactor size and operating costs. The requirements for a good oxygen carrier are high oxygen transport capacity, high reactivity, high mechanical strength, environmental friendliness, physical and chemical stability during cyclic tests, and low carrier production costs.[6] The metal oxides of Ni, Cu, Fe, Co, and Mn have been tested by various researchers at different scales.[7−11] Generally, these metal oxides are combined with an inert material that acts as a support, such as Al_2O_3, $MgAl_2O_4$, ZrO_2, and TiO_2, to enhance the surface area and durability of the oxygen carrier particles.

Fe_2O_3 has been studied as an oxygen carrier in the past; however, a slow reaction rate with CH_4 is a known issue with Fe_2O_3-based carriers. It is also known that impregnated Fe_2O_3 on alumina exhibits high reactivity with CH_4.[12] One of the goals in oxygen carrier development is to increase the efficiency of the release of oxygen of Fe_2O_3 during both the reduction and oxidation reactions. The complete combustion of the fuels results in the reactor effluent containing only CO_2 and H_2O, whereas the partial combustion produces the CO and H_2 products. The potential benefit of increasing the oxygen use at the Fe_2O_3 reaction site would be to increase the rate of conversion and to achieve a more complete combustion of the fuel, thereby improving the performance of the oxygen carrier.

In our laboratory experiments, we have studied the ability of cerium oxide to enhance the performance of the natural ore hematite (Fe_2O_3) during the CLC reaction. It has been reported that ceria appears to enhance the catalytic activity of the Group VIII metals, and some have suggested that ceria may actually alter the properties of the Group VIII metals.[13−15] The oxygen storage capacity of ceria and ceria–zirconia has been established as a key parameter for the catalytic performance of three-way catalysts.[16−23] Various studies previously conducted have used ceria as a support material for dispersing the active catalytic components as well as an oxygen transfer material for catalytic reactions. For example, the Rh/ceria catalyst is reported to have a high activity for the water-gas shift reaction, because of cerium aiding the removal of CO at lower

Special Issue: Accelerating Fossil Energy Technology Development through Integrated Computation and Experiment

Received: December 20, 2012
Revised: February 27, 2013
Published: February 28, 2013

   dx.doi.org/10.1021/ef302132e | *Energy Fuels* 2013, 27, 4087−4096

temperatures.[23−26] The studies described in this paper have demonstrated that the addition of a small amount of cerium (5 and 25%) to the hematite ore does not increase the surface area of the hematite carrier but significantly enhances the oxygen use of the oxygen carrier. Additionally, the studies have also indicated that CeO_2 promotes the CLC reaction and does not act as a support to the oxygen carrier.

This research work is aimed at studying the mechanism of methane CLC using Fe_2O_3 promoted with cerium oxide. The studies were conducted through thermogravimetric analysis (TGA) and a lab-scale flow reactor operated in both the continuous and pulsed flow modes. A fundamental understanding of the reaction pathway could help in guiding the future preparations of the desired oxygen carriers for more efficient oxygen use and CO_2 selectivity during the methane CLC process.

2. EXPERIMENTAL SECTION

2.1. Materials and Oxygen Carrier Preparation. The Michigan hematite used for these studies was supplied by Ward's Natural Science, Rochester, NY. Grade-2.0 helium, used as a purge gas between oxidation and reduction cycles, was obtained from Butler Gas Products Co., Inc. The ultrahigh-purity (UHP)-grade CH_4, used for the reduction cycle, was obtained from Matheson Trigas. N_2/O_2 (air) used for the oxidation cycle was obtained from Butler Gas Products Co., Inc.

In the study, the oxygen carriers were prepared by the hot incipient wetness impregnation method. The hematite was ground prior to incorporation of the CeO_2 promoter with a mortar and pestle and sieved to 150 μm. The pure cerium oxide material was obtained by calcining cerium nitrate (Aldrich) in a furnace at 800 °C. In the hot incipient wetness impregnation method, a saturated aqueous solution of cerium nitrate was prepared corresponding to the desired 5% (2.91 M) and 25% (8.545 M) loading of CeO_2 and was added dropwise to the hematite. The 5% CeO_2/hematite carrier (100 g sample) required one impregnation step, followed by calcination at 850 °C for 3 h. The 25% CeO_2/hematite carrier (100 g sample) required 6 impregnation steps, with intermediate drying at 100 °C. The resulting solid material was calcined at 850 °C for 3 h. For comparison purposes, 5 and 25% Al_2O_3/hematite were also prepared by the impregnation method. The Brunauer−Emmett−Teller (BET) surface area and pore size of the oxygen carriers were measured using a Micromeritics ASP-2020 apparatus.

2.2. Fixed-Bed Lab-Scale Reactor Study. The oxidation and reduction studies were carried out using a Micromeritics AutochemHP lab-scale quartz reactor. The fixed-bed lab-scale flow reactor was operated in both continuous and pulsed flow modes. Approximately 1.0 g of sample was placed in the quartz glass reactor coupled with a Pfeiffer Omnistar mass spectrometer (MS). The reactor effluent was monitored for the molecular ion responses corresponding to CH_4 (m/z 16), H_2O (m/z 18), CO (m/z 28), O_2 (m/z 32), Ar (m/z 40), and CO_2 (m/z 44). During the continuous flow mode, the inlet flow of 100% Ar was maintained at a total flow rate of 60 cm^3/min (space velocity of 2300 h^{-1}) over the oxygen carrier at 101.3 kPa while heating from 25 to 800 °C at a heating rate of 10 °C/min. The reactor temperature was maintained at 800 °C during the oxidation (air, 60 cm^3/min, 30 min) and reduction (20% CH_4/balance Ar, 60 cm^3/min, 30 min) cycles. During the pulse flow mode, the reduction (100% CH_4) and oxidation (air) periods were divided into 15 pulses (5 cm^3) into an argon flow (60 cm^3/min) over approximately 1.0 g of oxygen carrier at 800 °C. Integrated molecular ion peaks for CO_2 and CO were used for calculating the oxygen transfer capacity of the oxygen carriers.

2.3. TGA. TGA was conducted in a TA Instruments model 2050 thermogravimetric analyzer. The samples were placed in a 5 mm deep and 10 mm diameter crucible. Approximately 80 mg of the metal oxide oxygen carrier was heated in a quartz bowl from ambient temperature to 800 °C at a heating rate of 10 °C/min under N_2 gas at a flow rate of 100 cm^3/min. The sample temperature was maintained isothermally for 20 min prior to the reduction and oxidation cycles. The reaction gases used during reduction were 20% CH_4/balance N_2, and air at a total flow rate of 100 cm^3/min was used during oxidation.

The mass-based reduction rate was calculated by first extracting the thermogram profile during the reduction cycle and converting the data to the fractional reduction (X) defined by eq 1

$$X = \frac{M_o - M}{M_o - M_f} \quad (1)$$

where M is the instantaneous weight of the metal oxide, M_o is the initial weight before reduction, and M_f is the final weight of the carrier after reduction for 30 min. The mass-based reduction rate was then calculated from eq 2

$$\text{global rate} = \frac{dX}{dt} \quad (2)$$

3. RESULTS

3.1. Oxidation−Reduction Experiments in the Lab-Scale Reactor. The data in Figure 1 compares the outlet concentrations in moles of CO_2 and moles of CO per 100 g of carrier as a function of reduction cycles at 800 °C for the 5 wt % CeO_2/hematite, 5 wt % Al_2O_3/hematite, and pure hematite (Figure 1a) and 25 wt % CeO_2/hematite, 25 wt % Al_2O_3/hematite, and pure hematite oxygen carriers (Figure 1b). The sequence of CLC reduction/oxidation cycles performed demonstrates that the oxygen carriers are all stable over multiple reduction and oxidation cycles. In addition to this, the reactivity slightly increased with the number of cycles for both the hematite and promoted hematite oxygen carriers. The pure hematite produced 0.12 mol of CO_2 on the second cycle and 0.17 mol of CO_2 after 15 reduction cycles. The lab-scale reactor data show the addition of 5% CeO_2 to the hematite increased the amount of CO_2 produced to 0.30 mol, increasing the oxygen use by 1.8 times, as compared to the pure hematite material after 15 reduction cycles. The pure hematite produced 0.03 mol of CO on the 15th reduction cycle, shown in Figure 1a. The addition of 5% CeO_2 to hematite also decreased the

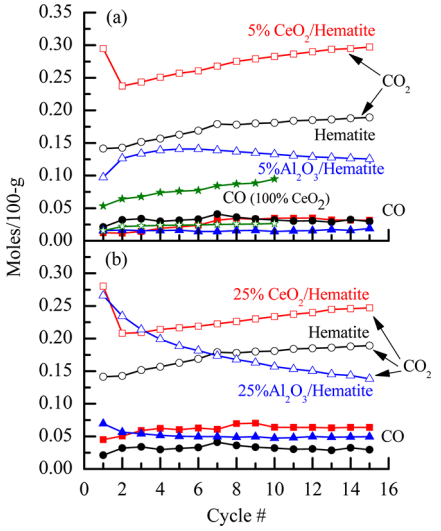

Figure 1. Amount of CO_2 (open symbols) and CO (closed symbols) produced during the reduction cycles flowing 20% CH_4/He at 800 °C over (a) 5% CeO_2/hematite, 5% Al_2O_3/hematite and hematite and (b) 25% CeO_2/hematite, 25% Al_2O_3/hematite, and pure hematite oxygen carriers.

dx.doi.org/10.1021/ef302132e | Energy Fuels 2013, 27, 4087−4096

amount of CO produced to 0.09 mol on cycle 2 and improved the selectivity for CO_2 over CO significantly. For comparison, a 5% Al_2O_3/hematite was prepared and tested for 15 oxidation and reduction cycles. The results are shown in Figure 1a. The data indicates that the addition of 5% Al_2O_3 decreased the amount of CO_2 produced to 0.10 mol of CO_2 from 0.12 mol (hematite) and the amount of CO produced was 0.017 mol on the second cycle. The decrease in CO_2 production, upon addition of 5% Al_2O_3, as compared to that with CeO_2, suggests Al_2O_3 does not participate in promoting combustion of CH_4. The addition of either Al_2O_3 or CeO_2 did not increase the surface area (CeO_2/hematite < 1.0 m^2/g) of the oxygen carrier (as shown in Table 1). The improvement in oxygen carrier

Table 1. BET Surface Areas of Oxygen Carriers

carrier	fresh (m^2/g)	reacted (m^2/g)	pore size[a] (Å)
CeO_2 (nitrate)	4.8		193.2
Fe_2O_3 (hematite)	<1.0	<1.0	63.6
5% Al_2O_3/Fe_2O_3	1.3	<1.0	67.0
25% Al_2O_3/Fe_2O_3	1.6	<1.0	129.4
5% CeO_2/Fe_2O_3	<1.0	<1.0	154.8
25% CeO_2/Fe_2O_3	<1.0	<1.0	306.1

[a]Freshly prepared materials.

capacity upon addition of CeO_2, during the CH_4 CLC, has to occur by a mechanism other than that of surface area enhancement. The fixed-bed multicycle tests of the pure CeO_2 produced 0.027 mol of CO_2 and 0.10 mol of CO on cycle 15. MS analysis indicates that the addition of 5 wt % CeO_2 to hematite oxygen carrier produces almost twice as much carbon dioxide per unit time in comparison to the sum of carbon dioxide produced when the Fe and Ce oxides are tested separately.

The 25% CeO_2/hematite oxygen carrier (Figure 1b) produced 0.24 mol of CO_2 and 0.06 mol of CO at 800 °C. Increasing the loading of CeO_2 decreased the amount of CO_2 produced (0.24 mol) as a result of the decrease in the Fe_2O_3 content, as compared to the 5% CeO_2/hematite carrier shown in Figure 1a. The additional CeO_2 also increased the amount of CO produced from 0.03 to 0.06 mol. For comparison, 25% Al_2O_3/hematite was prepared and tested; multicycle tests reveal that increasing the Al_2O_3 loading to 25% significantly increased the amount of CO_2 produced to 0.23 mol in cycle 2 and increased the amount of CO produced slightly to 0.047 mol, as compared to the pure hematite sample. The first reduction cycle of the 25% Al_2O_3/hematite carrier is comparable to the 25% CeO_2/hematite carrier. However, after multiple redox cycles, the carrier with 25% Al_2O_3 shows significant deactivation, and at the end of 15 cycles, the capacity was less than that of the pure hematite.

The oxygen transfer capacity of the CeO_2/Fe_2O_3 oxygen carriers was determined using the molecular ion profiles for CO_2 and CO monitored during the CLC reduction cycles at 800 °C. Panels a and b of Figure 2 show the percent oxygen used during the reduction cycles at 800 °C for the 5 and 25% CeO_2/hematite, respectively. The percent oxygen used was calculated according to eq 3

$$\text{percent } O_2 \text{ utilization} = \frac{n_{O_2}}{n_{O_2}\,(\text{theoretical})} \qquad (3)$$

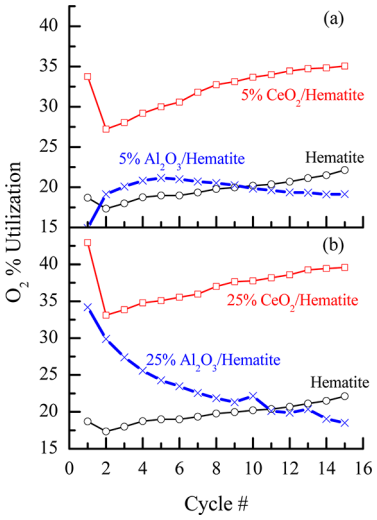

Figure 2. Percent oxygen utilization during the reduction cycles flowing 20% CH_4/He at 800 °C over (a) 5% CeO_2/hematite, 5% Al_2O_3/hematite, and pure hematite and (b) 25% CeO_2/hematite, 25% Al_2O_3/hematite, and pure hematite oxygen carriers.

where n_{O_2} is the moles of oxygen used during the reduction reaction to form CO and CO_2. Inductively coupled plasma mass spectroscopy (Galbraith Laboratories) and Material Safety Data Sheet (MSDS) data indicated that 99% of hematite is Fe_2O_3; this value was used for calculation of n_{O_2} (theoretical), the theoretical total amount of oxygen available in the oxygen carrier. The amount of oxygen used on the pure hematite oxygen carrier, during the 30 min reduction time during the 15 cycle test, is between 18.5 and 22.1% O_2 (Table 2). The addition of 5% cerium, by impregnation, to the hematite material resulted in an increase in O_2 utilization to 35.2%, and this corresponds to an increase in 13.1% utilization of oxygen, as compared to pure hematite. Adding 5% Al_2O_3 to hematite did not have any significant impact on oxygen utilization of hematite.

The surface area increase with the 5% CeO_2 was minimal (see Table 1), yet the increase in oxygen transfer capacity (Table 3) was very significant, indicating that the mechanism of promotion by CeO_2 is due to a chemical effect and not a surface area effect. The 25% CeO_2/hematite carriers, shown in Figure 2b, also show an improvement in the amount of oxygen used during the reduction cycles. It is interesting to note that increasing the amount of cerium oxide percentage from 5 to 25 wt % did not significantly improve the amount of oxygen used during the reduction cycle. Results with the 25% Al_2O_3/hematite oxygen carrier for multicycle testing are shown in Figure 2b. The 25% Al_2O_3/hematite carrier shows 34.6% oxygen availability in cycle 1 for the reduction reaction; however, significant deactivation occurred over 15 cycles that resulted in only 18.7% O_2 being available for oxidation, which is less than that of the pure hematite carrier and similar to the 5% Al_2O_3/hematite carrier. The addition of 25% CeO_2 to hematite improved the oxygen utilization of hematite, and it was stable during the 15 cycle test, unlike the 25% Al_2O_3/hematite. The results of the lab-scale reactor study demonstrate that the reactivity and oxygen availability of the hematite carrier is improved by the addition of the cerium oxide additive; CeO_2 has a unique effect on promoting the performance of Fe_2O_3.

dx.doi.org/10.1021/ef302132e | Energy Fuels 2013, 27, 4087−4096

Table 2. Moles of CO_2 and CO and Percentage of O_2 Used per 100 g Carrier during the Bench-Scale Reactor Tests

	moles of CO_2/100 g		moles of CO/100 g		percentage of O_2 used
carrier	cycle 2	cycle 15	cycle 2	cycle 15	cycle 15
hematite	0.12	0.17	0.032	0.032	22.2
5% CeO_2/hematite	0.23	0.30	0.009	0.032	35.2
5% Al_2O_3/hematite	0.10	0.12	0.017	0.019	18.5
25% CeO_2/hematite	0.21	0.24	0.049	0.063	39.6
25% Al_2O_3/hematite	0.23	0.13	0.055	0.047	18.7
100% ceria	0.016	0.027	0.064	0.10	

Table 3. Oxygen Transfer Capacity (R_o) of the Oxygen Carriers

			R_o				
carrier	fuel	reactor	750 °C	800 °C	900 °C	CO_2 selectivity	reference
hematite	20% CH_4/N_2	fix bed	0.018	0.027	0.06	84[a]	this work
5% CeO_2/hematite	20% CH_4/N_2	fix bed	0.024	0.037	0.11	90[a]	this work
25% CeO_2/hematite	20% CH_4/N_2	fix bed	0.031	0.042	0.14	79[a]	this work
40% CuO/20% Fe_2O_3/Al_2O_3	20% CH_4/N_2	TGA		0.14	0.14		40
45% Fe_2O_3/Al_2O_3	15% CH_4	fluid bed			0.013[b]		10
60% Fe_2O_3/Al_2O_3	88% CH_4	fluid bed			0.031[b]	70[b]	28
15% Fe_2O_3/Al_2O_3	25% CH_4	fluid bed			0.015[b]	50[b]	12
40% NiO/Al_2O_3	15% CH_4	fluid bed			0.084[b]		10
10% CuO/Al_2O_3	15% CH_4	fluid bed			0.02[b]		10
40% NiO/$MgAl_2O_4$	50% CH_4, 50% H_2O	fluid bed			0.045[b]	90[b]	30
18% NiO/Al_2O_3	30% CH_4/N_2	TGA, fluid bed			0.038[b]	60[b]	29

[a]A 800 °C reaction temperature. [b]A 950 °C reaction temperature.

3.2. Reactivity of the Oxygen Carriers Investigated by TGA.

Figure 3a shows the rate of mass conversion as a function of the fractional mass conversion (ω) for the 2nd, 8th, and 15th reduction periods at 800 °C for the CeO_2-promoted hematite and pure hematite oxygen carriers computed from the TGA data. The pure hematite oxygen carrier shows a low reaction rate (0.30 min^{-1}, cycle 2), illustrating the slow reactivity of the carrier toward combustion of methane. The rate of reaction for hematite as a function of the cycle number is shown in Figure 3b for reduction cycles 2, 8, and 15, and the data indicate that the reactivity of hematite increased slightly with the increasing number of reduction cycles (to 0.76 min^{-1} on reduction cycle 15). The TGA thermogram profile for hematite showed only a 2.7% decrease in the carrier weight, following a 20 min reduction, indicating that Fe_2O_3 was not fully converted to Fe_3O_4. An important characteristic of the oxygen carrier is the oxygen transport capacity, also called the oxygen ratio,[10,27] defined as $R_o = (m_{ox} - m_{red})/m_{ox}$, where m_{ox} and m_{red} are the masses of the oxidized and reduced forms of the metal oxide, respectively. The oxygen transport capacity during 20 min of reduction for pure hematite oxygen carrier was 0.027. The addition of 5% CeO_2 to hematite significantly increased the reaction rate to 1.37 min^{-1} (Figure 3b) at low fractional coverage and, correspondingly, increased the oxygen transport capacity to 0.037. Increasing the loading of CeO_2 to 25% further increased the maximum reaction rate to 1.45 min^{-1} and the oxygen transport capacity to 0.042. Increasing the reaction temperature from 800 to 900 °C significantly affected the reaction rate, producing a higher oxygen transfer capacity than that of the pure hematite carrier, as shown in Table 3. It is interesting to note that the oxygen transfer capacity of the promoted carriers is better than that reported for other iron-based carriers.[10,12,28]

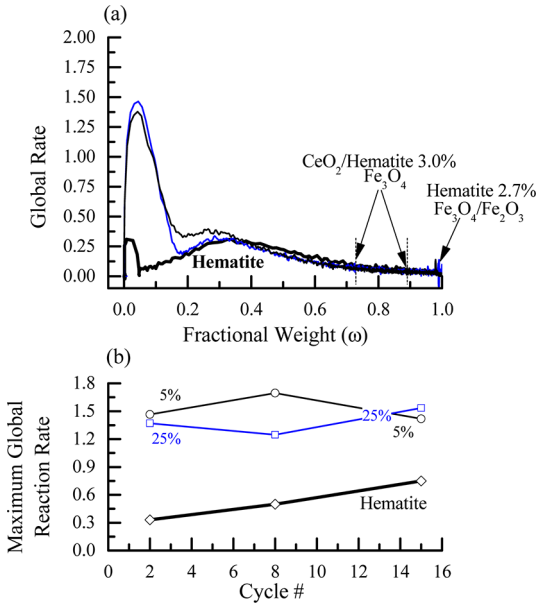

Figure 3. Reaction rates from TGA data at 800 °C as a function of the (a) mass-based conversion and (b) cycle number.

Initially, CH_4 reacts very rapidly with the oxygen carrier, indicated by a sharp increase in the rate and a more gradual decrease in the rate at higher exposure times. This effect may be due to two kinds of reactions taking place during the reduction of the oxygen carrier or the reaction of surface and bulk oxygen. The weight change of >3 wt % in thermogram profiles of the CeO_2-promoted hematite oxygen carriers indicates that CeO_2 improved the reducibility of the hematite material, converting all Fe_2O_3 to Fe_3O_4 in less than 20 min, and some Fe_3O_4 was also converted to FeO during the 20 min reduction time. Increasing the CeO_2 loading on hematite slightly increased the reactivity of the oxygen carrier, and hence, the conversion of

dx.doi.org/10.1021/ef302132e | Energy Fuels 2013, 27, 4087−4096

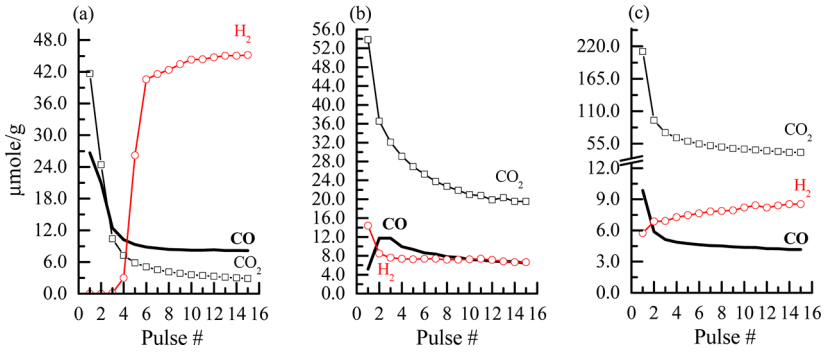

Figure 4. CH_4 pulses (5 cm^3) over (a) pure CeO_2, (b) pure hematite, and (c) 5% CeO_2/hematite oxygen carriers at 800 °C.

Fe_2O_3 to Fe_3O_4 was completed in a shorter time period (lower fractional weights), as shown in Figure 3b.

3.3. Pulsed Reaction Study in the Fixed-Bed Reactor. The pulse experiments were conducted, similar to other studies,[29,30] to investigate a smaller conversion range at a given time, as compared to that of the continuous flow experiment, to help elucidate the detailed reaction mechanism. The concentrations of products formed were determined from the volumetric fraction of each gas leaving the reactor during the exposure to 5 cm^3 methane. The concentration profile as a function of the pulse number at 800 °C is shown for the pure CeO_2 in Figure 4a. MS analysis of the reactor effluent shows that the second CH_4 pulse over the oxygen-rich CeO_2 at 800 °C produces CO, CO_2, H_2, and gaseous H_2O. Studies[31] have shown that the reduction of CeO_2 by CH_4 is thermodynamically favorable and the oxidation activity of ceria is dependent upon the oxidation state under the reaction condition at 800 °C. The high oxygen mobility of CeO_2 results in the initial formation of CO_2. Increasing the number of CH_4 pulses, the concentration profiles for CO, CO_2, and H_2 (see Figure 4a) indicate that oxygen is depleted from CeO_2 by the decrease in CO_2 production to near zero, followed by a steady-state formation of CO and H_2 through nine pulses. The reaction of CH_4 with the reduced CeO_{2-x} readily converts the reactant gas to CO and H_2. Following the decrease in CO_2 and slight decrease in the CO concentration, an increase in H_2 was observed. The decrease in the CO/H_2 ratio indicates that methane pyrolysis may be occurring, leading to carbon and H_2 formation according to reaction step 4.

$$CH_4 \xrightarrow{CeO_x} C + H_2O/H_2 \quad (>800\ ^\circ C) \tag{4}$$

The formation of carbon is verified by examining the molecular ion data during the oxidation cycle. The CO_2 molecular ion profiles show an increase in the CO_2 concentration when pulsing air (Figure 5a) on the reduced CeO_2 sample. A similar observation of CO_2 formation was also observed during the oxidation cycle of the continuous flow experiments (Figure 5b). The increase in the CO_2 concentration during oxidation indicates that carbon deposition occurred during the CH_4 reduction cycle on CeO_2. During the sequence of 15 air pulses (Figure 5a) on the reduced CeO_2 samples, the molecular ion profile of CO_2 shows an increasing trend initially followed by a decreasing trend. This suggests that the oxygen in the pulse is being consumed preferentially for oxidation of reduced cerium oxide initially. As the reduced cerium oxide is oxidized, more oxygen becomes available for reaction with carbon to form CO_2. Increasing the number of O_2 pulses shows a decrease in the amount of CO_2 formed as the carbon is consumed. The

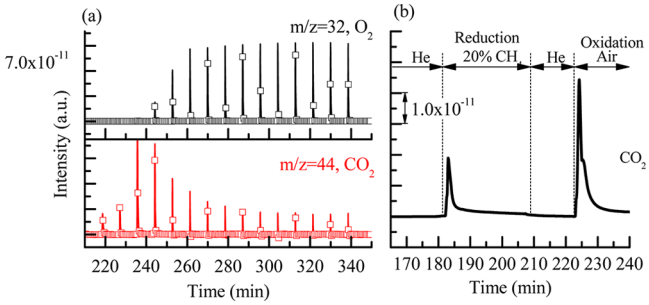

Figure 5. Molecular ion CO_2 profiles over the pure CeO_2 at 800 °C during (a) oxidation pulses and (b) reduction and oxidation cycles during continuous flow reactions.

continuous flow study (Figure 5b) indicates that 0.38 mmol of carbon was deposited during the reduction and remained on the carrier until its removal during oxidation.

The concentration profiles for the pure hematite oxygen carrier, during the CH_4 pulses at 800 °C, are displayed in Figure 4b. The second pulse of methane yielded mostly CO_2 (36.8 μmol) and some CO (11.7 μmol) and H_2 (8.5 μmol). The concentration profile for the hematite oxygen carrier is quite different from that of the pure CeO_2, in which CO was the main product. The hematite oxygen carrier continuously releases CO_2 as the conversion of CH_4 decreased with the increasing number of pulses. The reaction of CH_4 during the reduction of hematite also produces CO, H_2, and gaseous H_2O, as indicated from the molecular ion analysis of the reactor effluent. The pulse experiment reveals that the decrease in the amount of oxygen available in the Fe_2O_3 carrier lowers the amount of CO_2 produced but the amount of H_2 and CO produced remains relatively stable. The consumption of oxygen from Fe_2O_3 leads to a lower amount of oxygen available during subsequent reduction pulses. Methane combustion over the pure hematite oxygen carrier produces CO_2, CO, H_2, and H_2O indicated by the molecular ion analysis of the reactor effluent, suggesting that the formation of these product species is occurring by reaction steps 5−7.

$$CH_4 + 12Fe_2O_3 \rightarrow CO_2 + 8Fe_3O_4 + 2H_2O$$
$$\Delta H^\circ_{r,800\ ^\circ C} = 171.3\ \text{kJ/mol} \tag{5}$$

$$CH_4 + 3Fe_2O_3 \rightarrow CO + 2Fe_3O_4 + 2H_2$$
$$\Delta H^\circ_{r,800\ ^\circ C} = 221.1\ \text{kJ/mol} \tag{6}$$

dx.doi.org/10.1021/ef302132e | Energy Fuels 2013, 27, 4087−4096

$$CH_4 + Fe_3O_4 \rightarrow CO + 3FeO + 2H_2$$

$$\Delta H^{\circ}_{r,800\ ^{\circ}C} = 276.9\ \text{kJ/mol} \quad (7)$$

Thermodynamic analysis was performed using Factsage 6.0 for the reaction steps 5−7, and the results are shown in Figure 9. Positive Gibbs free energy values at lower temperatures indicate that the reaction with Fe_2O_3 is not thermodynamically favorable. However, all of the reactions are thermodynamically favorable above 700 °C.

The concentration profile in Figure 4b shows that, on pulses 12−15, the CO and H_2 concentration is similar. It is difficult to distinguish whether methane pyrolysis is occurring during the reduction cycle on the reduced iron oxide carrier. The formation of CO_2 (Figure 6a) from the reduced sample in the oxidation cycle during both the pulsed and continuous flow studies revealed that the formation of carbon did occur on the hematite oxygen carrier during the reduction reaction. The CO_2 molecular ion profile shows an increase in the CO_2 concentration while pulsing O_2 (Figure 6a) and also during the continuous flow oxidation with air, as shown in Figure 6b. The reduced hematite in Figure 6a required a greater number of O_2 pulses to reoxidize the oxygen lattice of the carrier, indicated by the O_2 pulse breakthrough occurring at pulse 9, as compared to pure CeO_2 (pulse 4). A similar CO_2 formation trend is observed while pulsing O_2 over the pure hematite, as compared to CeO_2. When the number of O_2 pulses is increased, there is an increasing amount of CO_2 produced, reaching a maximum, followed by a decrease in CO_2 production. The pulse study reveals that O_2 consumption for metal oxidation and carbon oxidation is occurring simultaneously over the hematite carrier.

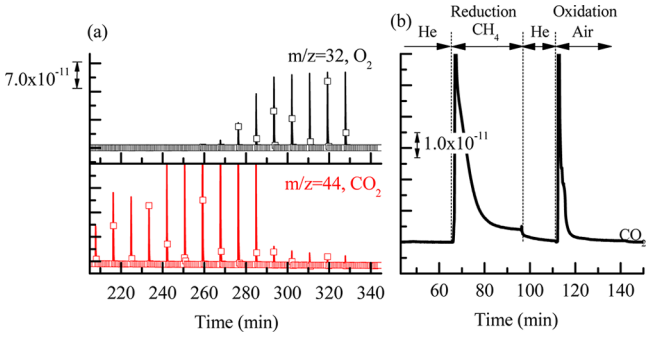

Figure 6. Molecular ion CO_2 profiles over the pure hematite oxygen carrier at 800 °C during (a) oxidation pulses and (b) reduction and oxidation cycles during continuous flow reactions.

The molecular ion profiles during the exposure to methane pulses over the 5% CeO_2/hematite oxygen carrier at 800 °C are shown in Figure 4c; the data indicate that the addition of CeO_2 to hematite significantly improves the conversion of CH_4 to CO_2. The CO_2 concentration decreases with an increasing number of pulses because of depletion of oxygen available for the reaction. The amount of CO formed decreased during the initial pulses, and then the amount of CO formed approached a steady state. Following the initial pulses, the H_2/CO selectivity changes, favoring the H_2 product, indicate that carbon formation is occurring over the oxygen-depleted surface of the oxygen carrier similar to pure CeO_2.

The oxidation pulses (see Figure 7a) over the reduced CeO_2/Fe_2O_3 sample indicate that less carbon remained

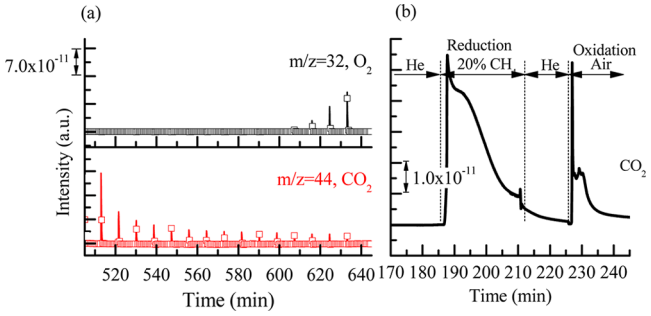

Figure 7. Molecular ion CO_2 profiles over the 5% CeO_2/hematite oxygen carrier at 800 °C during (a) oxidation pulses and (b) reduction and oxidation cycles during continuous flow reactions.

deposited on the oxygen carrier than that of the pure hematite or pure CeO_2. These results suggest that carbon may also be readily reacting with iron oxide via the solid−solid reaction to form CO_2. The carbon that was formed during each pulse had sufficient time to react with the oxygen present in Fe_2O_3 before the next pulse, resulting in less carbon deposited on the CeO_2/Fe_2O_3 carrier. In addition to this, the CO_2 molecular ion profiles (Figure 7a) do not show the increasing and decreasing trend as pure CeO_2 (Figure 5a) and pure hematite (Figure 6a), suggesting that the majority of the carbon formed by pyrolysis reacted with the oxygen carrier at the active sites during the reduction cycle. The O_2 pulse study also reveals that the presence of CeO_2 increased the oxygen utilization of Fe_2O_3, as indicated by the high O_2 consumption, before the O_2 pulse breakthrough is observed. The pulse study indicates that CeO_2/Fe_2O_3 decreased the amount of carbon deposition and increased the amount of O_2 utilization.

3.5. Temperature-Programmed Reaction (TPR) in 5, 10, and 20% CH_4. The data presented in Figure 8 show the CO_2 and CO molecular ion profiles while flowing 5, 10, and 20% CH_4 over the 25% CeO_2/hematite and pure hematite oxygen carriers while heating from 25 to 950 °C. While flowing 5% CH_4 over the pure hematite oxygen carrier (shown in Figure 8a), the conversion of CH_4 to CO_2 begins at around 700 °C over the pure hematite and peaks at 950 °C. The hematite oxygen carrier produced very little CO even at 950 °C. The hematite carrier shows initial CO_2 and CO peaks at 700 °C (low T), indicating that CH_4 is reacting with the oxygen species located on the surface of the oxygen carrier. Surface oxygen generally has a higher activity at lower temperatures than the bulk oxygen activity at higher temperatures.[32] Increasing the temperature of the reaction from 700 °C, CH_4 and Fe_2O_3 react to form more CO_2 beginning at 750 °C, with a maximum at 950 °C. As O_2 is depleted from the hematite carrier, the CO_2 molecular ion intensity decreases. At higher temperatures, with carbon formation by pyrolysis of CH_4, the carbon remains upon the surface of the hematite carrier, unreacted. The CO_2 molecular ion profile for the CeO_2/Fe_2O_3 carrier shows that CO_2 formation also begins at 700 °C and CeO_2 promotes a significantly larger amount of CO_2 that peaks at 825 °C. When the exposure time of 5% CH_4 is increased to the CeO_2/Fe_2O_3 carrier at 950 °C, there is a second increase in the CO and CO_2 molecular ion profiles, indicating the formation of these species. The carbon produced at a high temperature over the reduced carrier reacts with the bulk Fe_2O_3 to form the CO_2 and CO product species. At higher temperatures, it appears that CeO_2 promotes more carbon that is able to react with Fe_2O_3 to form a greater amount of CO_2 along with the partial oxidation

dx.doi.org/10.1021/ef302132e | Energy Fuels 2013, 27, 4087−4096

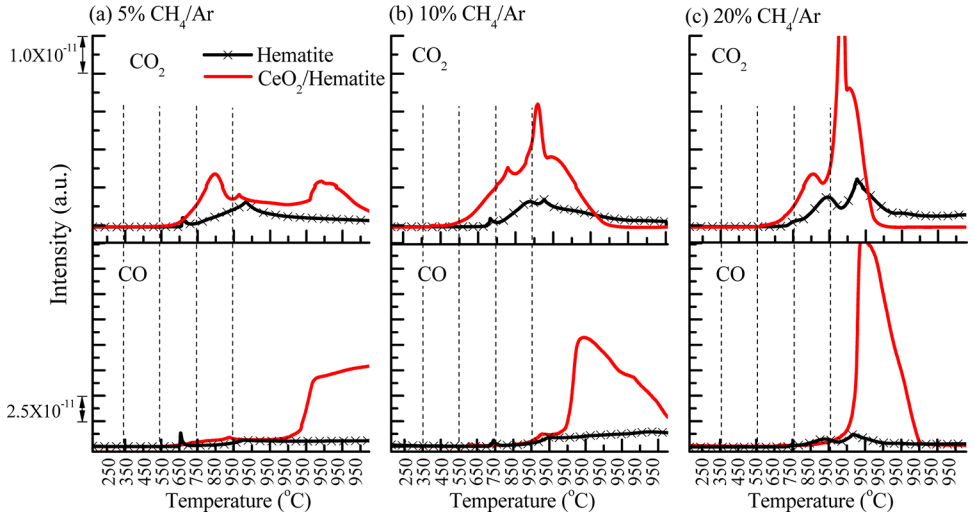

Figure 8. Molecular ion analysis during TPR of hematite and 25% CeO_2/hematite while heating from 25 to 950 °C under (a) 5% CH_4/Ar flow, (b) 10% CH_4/Ar flow, and (c) 20% CH_4/Ar flow.

product CO upon depletion of the available oxygen in the carrier. It is interesting that this two-peak phenomenon in the CO_2 molecular ion TPR profiles is still observable with an increased methane concentration.

Increasing the reactant concentration to 10% CH_4 (Figure 8b) and 20% CH_4 (Figure 8c) causes an increase in the CO_2 product over all of the oxygen carriers. It is interesting that, at higher CH_4 concentrations, the second CO_2 peak was observed at a shorter reaction time for the CeO_2/Fe_2O_3 carrier. This effect is likely due to the fact that, at higher concentrations, there will be a greater amount of carbon formed in a shorter time than is available for reaction with the bulk Fe_2O_3. The larger amount of carbon present will react more readily with Fe_2O_3, thus shifting the CO_2 molecular ion profile forward on the time scale, as compared to the TPR profile for the 5% CH_4 test. Upon depletion of the oxygen available in the CeO_2/Fe_2O_3 carrier, it is possible to observe carbon partially oxidizing to the CO product species.

When pure hematite was exposed to 20% CH_4 (Figure 8c), the characteristic two-peak CO_2 molecular ion profile, like that of the CeO_2/Fe_2O_3 carrier tested, can be observed. The emergence of the two CO_2 peaks is indicative of the carbon formation pathway for CO_2 that is evident in the CeO_2/Fe_2O_3 carrier. Increasing the concentration of CH_4 increases the amount of carbon formed on the pure hematite carrier. The larger amount of carbon at a high temperature (950 °C) may be capable of oxidizing the bulk Fe_2O_3 to produce a larger amount of CO_2 and corresponding second CO_2 peak. The formation of the CO molecular ion profile also moves through a maximum (Figure 8c), indicating that carbon formation and oxidation may be the reaction pathway; as carbon is depleted, the amount of CO formed decreases, unlike the CO profiles at the 5 and 10% CH_4 concentrations (shown in panels a and b of Figure 8, respectively).

The TPR data indicate that the addition of CeO_2 to hematite increased the amount of CO_2 formed. Interestingly, the TPR experiments suggest that carbon reacting with the bulk oxygen may be responsible for the formation of a larger amount of CO_2 and some CO on the depletion of the available oxygen in the oxygen carrier. The CO_2 molecular ion profile during the 5% CH_4 TPR (Figure 8a) over the CeO_2-promoted hematite carrier shows two peaks for CO_2 formation, the first at 850 °C and the second at 950 °C. The first peak does not correspond to the formation of CO, indicating that the lower temperature formation of CO/H_2 is reacting with Fe_2O_3 to form CO_2. The pulsed experiments and TPR data indicate that the addition of CeO_2 to hematite increases the amount of oxygen available for combustion of CH_4, and a major reaction pathway is that of the formation of carbon and oxidation by the oxygen carrier.

4. DISCUSSION

In the CLC process, the degree of fuel combustion has to be high to achieve full conversion of methane to CO_2 and H_2O. Ideally, the exit stream of the reactor should be composed of mostly CO_2 and H_2O. The oxygen required to obtain full combustion of CH_4 must be supplied from the oxygen carrier in the fuel reactor. For methane combustion to occur, there must be a rapid transfer of oxygen from the metal oxide surface to methane. The continuous flow lab-scale reactor tests revealed that hematite is capable of transferring oxygen to the methane gas to produce CO_2 and CO (Figure 1a). The addition of 5 and 25% ceria oxide to hematite significantly increased the amount of CO_2 produced, as compared to the pure hematite oxygen carrier. The addition of 5 and 25% CeO_2 to hematite showed higher reactivity than the pure hematite oxygen carrier for methane combustion. In addition to the reaction rate increase, the addition of 5% CeO_2 almost doubled the amount of oxygen used during the reduction reaction. The amount of oxygen supplied by CeO_2 alone is not sufficient for this significant increase in combustion, suggesting that the ability of cerium oxides for partial oxidation of methane may be a key factor.

The global reaction rate data, shown in Figure 3a, for the hematite oxygen carrier shows two peaks corresponding to two regions of high activity. The change in the combustion performance is related to the reduction state of the oxygen carrier at any given time. During the TPR studies, the formation of a CO_2 peak at a low temperature on Fe_2O_3 may be attributed to the surface reaction (Figure 8). The emergence of a second peak at a higher temperature (Figure 8) may be attributed to iron oxide reduction, occurring from the oxidation of carbon. The pure hematite is limited by its reactivity (Figure 3a) and less than 3% of the oxygen in the carrier is available for the CLC reduction reaction in short time periods (20 min).

dx.doi.org/10.1021/ef302132e | Energy Fuels 2013, 27, 4087−4096

The addition of CeO_2 to Fe_2O_3 shifted the CO_2 peaks to lower temperatures while producing more CO_2 than the pure hematite oxygen carrier during the TPR experiments while flowing 5, 10, and 20% CH_4 (as shown in panels a, b, and c of Figure 8, respectively), demonstrating the ability of ceria as a promoter to increase the amount of available oxygen during the reduction reaction.

X-ray diffraction analysis (not shown) of the CeO_2/Fe_2O_3 oxygen carriers showed that there was no formation of Ce−Fe alloys or mixed Ce−Fe−O compounds. Following 15 oxidation and reduction cycles, the oxidized forms of the carrier show that CeO_2 and Fe_2O_3 remained as separate phases. Therefore, it is assumed that the high activity of the CeO_2/Fe_2O_3 carrier is due to the cooperative participation of CeO_x sites, which produce intermediate species CO, H_2, and carbon that facilitate further reduction of the iron oxide carrier.

Cerium oxide is reported as having a high oxygen mobility (redox property)[21] and high oxygen storage capacity,[16,20,22,33−35] which is affected by the strong interaction of cerium with the support metal (strong metal−support interaction).[36] It has been reported that, at high temperatures, the lattice oxygen at the CeO_2 surface can also partially oxidize gaseous hydrocarbons, such as methane.[37,38] Incorporation of CeO_2 into the hematite material (panels a and b of Figure 1) increased the O_2 utilization of Fe_2O_3 (panels a and b of Figure 2). A large amount of the available oxygen in CeO_2 contributed to the partial oxidation of methane to form carbon monoxide and to the formation of carbon. This suggests that CeO_2 may act as an active site for initial methane partial oxidation to form CO and H_2 and Fe_2O_3 as the site for further oxidation of CO and H_2 to produce CO_2 and H_2O. The advantage of the impregnation method is the deposition of CeO_2 particles directly onto the Fe_2O_3 active site, where the partial oxidation products may readily react with the oxygen-rich Fe_2O_3 in the hematite carrier. A larger amount of CO_2 formation is achieved by the dual function Fe_2O_3−CeO_2 mixed carrier.

The MS analysis of the pulse transient experiments (Figure 4c) conducted over the 5% CeO_2/hematite carrier in the fixed-bed reactor at 800 °C suggests that carbon formation is occurring at the later part of the reaction, indicated by the decrease in the CO concentration and increase in the H_2 concentration. This is also confirmed by the CO_2 formation during oxidation of the reduced CeO_2. The formation of carbon is most likely occurring at the reduced CeO_x sites. Because of the high temperature range used in the CLC process (750−900 °C), carbon formation via the decomposition of hydrocarbons over the reduced metal oxides is highly favorable thermodynamically[39] and reduced metal oxides are known to catalyze this reaction. The pulse study revealed that less carbon was formed in the CeO_2/Fe_2O_3 mixed carrier, and this is consistent with the greater amount of O_2 that was used and larger amount of CO_2 produced. The reaction of carbon with Fe_2O_3 is thermodynamically favorable because the combustion reaction took place above 700 °C (Figure 9). These results suggest that carbon formed on the reduced CeO_2 may be readily oxidized by the iron oxide that is in the vicinity of CeO_2.

This study has revealed that the redox mechanism of CeO_2 and Fe_2O_3 may provide an important link in enhancing the combustion of CH_4 for the CLC reaction. CeO_2 that is in the vicinity of Fe_2O_3 can impact the oxidation behavior of Fe_2O_3. The improvement in performance upon the addition of CeO_2 results in higher rates of CH_4 decomposition and subsequent oxidation of decomposition products, such as carbon, CO, and

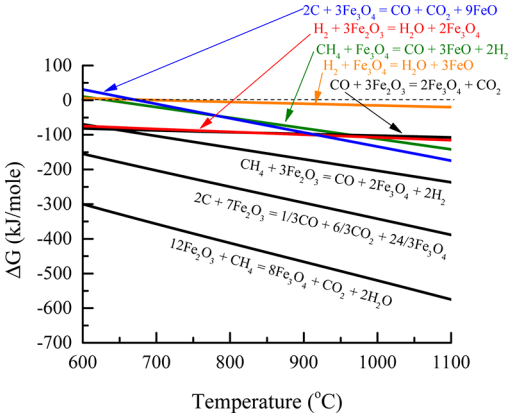

Figure 9. Thermodynamic analysis (ΔG versus temperature) of CH_4, CO, and H_2 combustion reactions with Fe_2O_3 and Fe_3O_4.

H_2, resulting in increased oxygen utilization during the CLC reduction reaction with Fe_2O_3. The key feature of CeO_2 is to improve the reactivity of hematite as a promoter but not act as a support material upon increasing the surface area. Thus, the promotion effect of CeO_2 on hematite may be due to the conversion of CH_4 to active intermediates that readily react with Fe_2O_3. The possible reaction mechanism is summarized below.

Partial oxidation of CH_4 on oxidized CeO_2:

$$CH_4 + 2CeO_2 \rightarrow CO + 2CeO_x + H_2 \text{ or } H_2O \quad (9)$$

$$CO + 3Fe_2O_3 \rightarrow 2Fe_3O_4 + CO_2$$
$$\Delta H^{\circ}_{r,800\ ^{\circ}C} = -39.3\ \text{kJ/mol} \quad (10)$$

$$H_2 + 3Fe_2O_3 \rightarrow H_2O + 2Fe_3O_4$$
$$\Delta H^{\circ}_{r,800\ ^{\circ}C} = -5.3\ \text{kJ/mol} \quad (11)$$

Methane decomposition on reduced CeO_x:

$$CH_4 \xrightarrow{CeO_x} C + H_2 \quad (12)$$

$$2C + 7Fe_2O_3 \rightarrow \frac{6}{3}CO + \frac{1}{3}CO_2 + \frac{24}{3}Fe_3O_4$$
$$\Delta H^{\circ}_{r,800\ ^{\circ}C} = 248.1\ \text{kJ/mol} \quad (13)$$

$$2C + 3Fe_3O_4 \rightarrow CO + CO_2 + 9FeO$$
$$\Delta H^{\circ}_{r,800\ ^{\circ}C} = 389.1\ \text{kJ/mol} \quad (14)$$

$$H_2 + 3Fe_2O_3 \rightarrow H_2O + 2Fe_3O_4$$
$$\Delta H^{\circ}_{r,800\ ^{\circ}C} = -5.3\ \text{kJ/mol} \quad (15)$$

$$H_2 + Fe_3O_4 \rightarrow H_2O + 3FeO$$
$$\Delta H^{\circ}_{r,800\ ^{\circ}C} = -50.5\ \text{kJ/mol} \quad (16)$$

Direct reaction of methane with Fe_2O_3:

$$CH_4 + Fe_2O_3 \rightarrow CO_2 + Fe_3O_4 + H_2O$$
$$\Delta H^{\circ}_{r,800\ ^{\circ}C} = 171.3\ \text{kJ/mol} \quad (17)$$

dx.doi.org/10.1021/ef302132e | Energy Fuels 2013, 27, 4087−4096

5. CONCLUSION

The CLC process is a technique that involves the use of metal oxide as an oxygen carrier, which transfers the oxygen from the air to the fuel. The addition of 5% CeO_2 to the hematite carrier significantly improved the amount of CO_2 produced, as compared to the pure hematite oxygen carrier. The surface area changes were minimal because of the addition of CeO_2; therefore, the promotion is due to a chemical effect. The addition of CeO_2 enhanced the rates of reduction of Fe_2O_3 significantly and is consistent with the improvement in the amount of oxygen available for reaction. The present results suggest that CeO_2 as an additive to hematite is very effective in improving the oxygen carrier performance of the natural ore hematite in the CLC reaction. The product analysis during continuous and pulsed flow reactor studies revealed that CeO_2 initially forms CO by partial oxidation of methane and CH_4 decomposition takes place on the reduced Ce_xO_y. When Fe_2O_3 is present in the vicinity of CeO_2, CO and carbon formed may be readily converted to CO_2. The pulsed flow reactor study also indicated that carbon and H_2 are formed by the decomposition of CH_4 upon reduced CeO_x that may also be converted to CO, CO_2, and H_2O by Fe_2O_3/Fe_3O_4. Therefore, in addition to the direct reaction of Fe_2O_3 with CH_4, the presence of CeO_2 promotes the formation of reactive intermediates that facilitate a greater use of oxygen from the natural ore hematite.

■ AUTHOR INFORMATION

Corresponding Author

*Telephone: +01-304-285-5292. Fax: +01-304-285-4403. E-mail: duane.miller@netl.doe.gov.

Notes

Disclaimer: This project was funded by the NETL, U.S. DOE, an agency of the United States Government, through a support contract with URS Energy and Construction, Inc. Neither the United States Government nor any agency thereof, nor any of their employees, nor URS Energy and Construction, Inc., nor any of their employees, makes any warranty, expressed or implied, or assumes any legal liability or responsibility for the accuracy, completeness, or usefulness of any information, apparatus, product, or process disclosed, or represents that its use would not infringe privately owned rights. Reference herein to any specific commercial product, process, or service by trade name, trademark, manufacturer, or otherwise does not necessarily constitute or imply its endorsement, recommendation, or favoring by the United States Government or any agency thereof. The views and opinions of authors expressed herein do not necessarily state or reflect those of the United States Government or any agency thereof.

The authors declare no competing financial interest.

■ ACKNOWLEDGMENTS

We thank Esmail Monazam for his help with the Gibbs energy calculations. This technical work was performed in support of NETL's ongoing research on CO_2 capture in the Separations and Fuels Processing Division (Project DE-FE0004000).

■ REFERENCES

(1) Kidambi, P. R.; Cleeton, J. P. E.; Scott, S. A.; Dennis, J. S.; Bohn, C. D. Interaction of iron oxide with alumina in a composite oxygen carrier during the production of hydrogen by chemical looping. *Energy Fuels* **2012**, *26*, 603.

(2) Gu, H. M.; Shen, L. H.; Xiao, J.; Zhang, S. W.; Song, T. Chemical looping combustion of biomass/coal with natural iron ore as oxygen carrier in a continuous reactor. *Energy Fuels* **2011**, *25*, 446.

(3) Azis, M. M.; Jerndal, E.; Leion, H.; Mattisson, T.; Lyngfelt, A. On the evaluation of synthetic and natural ilmenite using syngas as fuel in chemical-looping combustion (CLC). *Chem. Eng. Res. Des.* **2010**, *88*, 1505.

(4) Fossdal, A.; Bakken, E.; Oye, B. A.; Schoning, C.; Kaus, I.; Mokkelbost, T.; Larring, Y. Study of inexpensive oxygen carriers for chemical looping combustion. *Int. J. Greenhouse Gas Control* **2011**, *5*, 483.

(5) Pröll, T.; Mayer, K.; Bolhàr-Nordenkampf, J.; Kolbitsch, P.; Mattisson, T.; Lyngfelt, A.; Hofbauer, H. Natural minerals as oxygen carriers for chemical looping combustion in a dual circulating fluidized bed system. *Energy Procedia* **2009**, *1*, 27.

(6) Lyngfelt, A.; Leckner, B.; Mattisson, T. A fluidized-bed combustion process with inherent CO_2 separation; application of chemical-looping combustion. *Chem. Eng. Sci.* **2001**, *56*, 3101.

(7) Yang, S.; Kim, K.; Baek, J.-I.; Kim, J.-W.; Lee, J. B.; Ryu, C. K.; Lee, G. Spinel $Ni(Al,Fe)_2O_4$ solid solution as an oxygen carrier for chemical looping combustion. *Energy Fuels* **2012**, *26*, 4617.

(8) Adanez, J.; Abad, A.; Garcia-Labiano, F.; Gayan, P.; de Diego, L. F. Progress in chemical-looping combustion and reforming technologies. *Prog. Energy Combust. Sci.* **2012**, *38*, 215.

(9) Cho, P.; Mattisson, T.; Lyngfelt, A. Comparison of iron-, nickel-, copper- and manganese-based oxygen carriers for chemical-looping combustion. *Fuel* **2004**, *83*, 1215.

(10) Abad, A.; Adánez, J.; García-Labiano, F.; de Diego, L. F.; Gayán, P.; Celaya, J. Mapping of the range of operational conditions for Cu-, Fe-, and Ni-based oxygen carriers in chemical-looping combustion. *Chem. Eng. Sci.* **2007**, *62*, 533.

(11) Johansson, M.; Mattisson, T.; Lyngfelt, A. Investigation of Mn_3O_4 with stabilized ZrO_2 for chemical-looping combustion. *Chem. Eng. Res. Des.* **2006**, *84*, 807.

(12) Gayán, P.; Pans, M. A.; Ortiz, M.; Abad, A.; de Diego, L. F.; García-Labiano, F.; Adánez, J. Testing of a highly reactive impregnated Fe_2O_3/Al_2O_3 oxygen carrier for a SR−CLC system in a continuous CLC unit. *Fuel Process. Technol.* **2012**, *96*, 37.

(13) Nunan, J. G.; Robota, H. J.; Cohn, M. J.; Bradley, S. A. Physicochemical properties of Ce-containing three-way catalysts and the effect of Ce on catalyst activity. *J. Catal.* **1992**, *133*, 309.

(14) Meriaudeau, P.; Dutel, J. F.; Dufaux, M.; Naccache, C. Further investigation on metal−support interaction: TiO_2, CeO_2, SiO_2 supported platinum catalysts. *Stud. Surf. Sci. Catal.* **1982**, *11*, 95−104.

(15) Zhou, Y.; Nakashima, M.; White, J. M. Interaction of platinum with ceria and silica. *J. Phys. Chem.* **1988**, *92*, 812.

(16) Miki, T.; Ogawa, T.; Haneda, M.; Kakuta, N.; Ueno, A.; Tateishi, S.; Matsuura, S.; Sato, M. Enhanced oxygen storage capacity of cerium oxides in cerium dioxide/lanthanum sesquioxide/alumina containing precious metals. *J. Phys. Chem.* **1990**, *94*, 6464.

(17) Vlaic, G.; Di, M. R.; Fornasiero, P.; Fonda, E.; Kaspar, J.; Graziani, M. The CeO_2−ZrO_2 system: Redox properties and structural relationships. *Stud. Surf. Sci. Catal.* **1998**, *116*, 185.

(18) Kaspar, J.; Di, M. R.; Fornasiero, P.; Graziani, M.; Bradshaw, H.; Norman, C. Dependency of the oxygen storage capacity in zirconia−ceria solid solutions upon textural properties. *Top. Catal.* **2001**, *16/17*, 83.

(19) Duprez, D.; Descorme, C.; Birchem, T.; Rohart, E. Oxygen storage and mobility on model three-way catalysts. *Top. Catal.* **2001**, *16/17*, 49.

(20) Imamura, S.; Shono, M.; Okamoto, N.; Hamada, A.; Ishida, S. Effect of cerium on the mobility of oxygen on manganese oxides. *Appl. Catal., A* **1996**, *142*, 279.

(21) Fornasiero, P.; Balducci, G.; Di Monte, R.; Kašpar, J.; Sergo, V.; Gubitosa, G.; Ferrero, A.; Graziani, M. Modification of the redox behaviour of CeO_2 induced by structural doping with ZrO_2. *J. Catal.* **1996**, *164*, 173.

(22) Zafiris, G. S.; Gorte, R. J. Evidence for a second carbon monoxide oxidation mechanism on rhodium/ceria. *J. Catal.* **1993**, *143*, 86.
(23) Harrison, B.; Diwell, A. F.; Hallett, C. Promoting platinum metals by ceria. Metal−support interactions in autocatalysts. *Platinum Met. Rev.* **1988**, *32*, 73.
(24) Su, E. C.; Montreuil, C. N.; Rothschild, W. G. Oxygen storage capacity of monolith three-way catalysts. *Appl. Catal.* **1985**, *17*, 75.
(25) Schlatter, J. C.; Mitchell, P. J. Three-way catalyst response to transients. *Ind. Eng. Chem. Prod. Res. Dev.* **1980**, *19*, 288.
(26) Kim, G. Ceria-promoted three-way catalysts for auto exhaust emission control. *Ind. Eng. Chem. Prod. Res. Dev.* **1982**, *21*, 267.
(27) Mattisson, T.; Järdnäs, A.; Lyngfelt, A. Reactivity of some metal oxides supported on alumina with alternating methane and oxygen application for chemical-looping combustion. *Energy Fuels* **2003**, *17*, 643.
(28) Abad, A.; Mattisson, T.; Lyngfelt, A.; Johansson, M. The use of iron oxide as oxygen carrier in a chemical-looping reactor. *Fuel* **2007**, *86*, 1021.
(29) Dueso, C.; Abad, A.; García-Labiano, F.; de Diego, L. F.; Gayán, P.; Adánez, J.; Lyngfelt, A. Reactivity of a NiO/Al_2O_3 oxygen carrier prepared by impregnation for chemical-looping combustion. *Fuel* **2010**, *89*, 3399.
(30) Johansson, M.; Mattisson, T.; Lyngfelt, A.; Abad, A. Using continuous and pulse experiments to compare two promising nickel-based oxygen carriers for use in chemical-looping technologies. *Fuel* **2008**, *87*, 988.
(31) Jerndal, E.; Mattisson, T.; Lyngfelt, A. Thermal analysis of chemical-looping combustion. *Chem. Eng. Res. Des.* **2006**, *84*, 795.
(32) Baran, E. J. Structural chemistry and physicochemical properties of perovskite-like materials. *Catal. Today* **1990**, *8*, 133.
(33) Kacimi, S.; Barbier, J.; Taha, R.; Duprez, D. Oxygen storage capacity of promoted Rh/CeO_2 catalysts. Exceptional behavior of $RhCu/CeO_2$. *Catal. Lett.* **1993**, *22*, 343.
(34) Padeste, C.; Cant, N. W.; Trimm, D. L. The influence of water on the reduction and reoxidation of ceria. *Catal. Lett.* **1993**, *18*, 305.
(35) Zafiris, G. S.; Gorte, R. J. Evidence for low-temperature oxygen migration from ceria to rhodium. *J. Catal.* **1993**, *139*, 561.
(36) Fan, L.; Fujimoto, K. Reaction mechanism of methanol synthesis from carbon dioxide and hydrogen on ceria-supported palladium catalysts with SMSI effect. *J. Catal.* **1997**, *172*, 238.
(37) Laosiripojana, N.; Assabumrungrat, S. Catalytic dry reforming of methane over high surface area ceria. *Appl. Catal., B* **2005**, *60*, 107.
(38) Ramírez-Cabrera, E.; Atkinson, A.; Chadwick, D. Reactivity of ceria, Gd- and Nb-doped ceria to methane. *Appl. Catal., B* **2002**, *36*, 193.
(39) Armor, J. N. The multiple roles for catalysis in the production of H_2. *Appl. Catal., A* **1999**, *176*, 159.
(40) Siriwardane, R.; Tian, H.; Simonyi, T.; Poston, J. Synergetic effects of mixed copper−iron oxides oxygen carriers in chemical looping combustion. *Fuel* **2013**, DOI: 10.1016/j.fuel.2013.01.023.